Light and heavy transfer products in ^{58}Ni+^{208}Pb at the Coulomb barrier

L. Corradi, A. M. Vinodkumar, A. M. Stefanini, E. Fioretto, and G. Prete
Istituto Nazionale di Fisica Nucleare, Laboratori Nazionali di Legnaro, Via Romea 4, I-35020 Legnaro, Padova, Italy

S. Beghini, G. Montagnoli, and F. Scarlassara
*Dipartimento di Fisica, Universitá di Padova, and Istituto Nazionale di Fisica Nucleare Sezione di Padova, Via Marzolo 8,
I-35131 Padova, Italy*

G. Pollarolo and F. Cerutti
*Dipartimento di Fisica Teorica, Universitá di Torino, and Istituto Nazionale di Fisica Nucleare, Sezione di Torino, Via Pietro Giuria 1,
I-10125 Torino, Italy*

Aage Winther
The Niels Bohr Institute, Blegdamsvej 17 2100, Copenhagen, Denmark

Light and heavy reaction products in the ^{58}Ni+^{208}Pb system were measured at $E_{lab}=328.4$ MeV. Light products were identified with a time-of-flight magnetic spectrometer and heavy fragments with a multiwire parallel plate detector. From the kinematic coincidence the survival probability of the heavy fragments against fission was derived. Data are well described by semiclassical model calculations including, in addition to all one particle transfers, a proton pair-transfer mode with a macroscopic form factor.

I. INTRODUCTION

In low-energy heavy-ion collisions, the mass and charge distributions from multinucleon transfer reactions are dominated by a quasi-elastic mechanism, where the transfer of nucleons is governed by nuclear structure and Q-value matching conditions. In various systems (see, e.g., Refs. [1–6]) there is evidence, at least for the case of neutrons, that the main degrees of freedom in this regime are provided by single nucleon transfer modes, being the multinucleon transfer channels populated via a sequence of individual particles. The transfer of correlated nucleons, pairs or even clusters, are also considered as significant degrees of freedom [7]. A relevant but very poorly investigated aspect of these reactions is if the description given in terms of the above degrees of freedom suffices when large energy losses appear. In this case the primary yields can be modified in a significant way by secondary processes such as nucleon evaporation, since the Q values of the reaction get more and more negative as the number of transferred nucleons increases. The influence of secondary processes may be even more important for the heavy partner of the reaction due to fission. In addition to the mass and charge yields of the light transfer products, a determination of the survival probability against fission of the heavy targetlike fragments would help understanding how effectively multinucleon transfer reactions populate heavy nuclei [8,9].

The ^{58}Ni+^{208}Pb system is a good candidate for multinucleon transfer studies, since its Q-value matching conditions, close to optimum up to eight proton stripping, allows one to investigate the mass and charge distributions of the light reaction products and to check if the same transfer mechanism is suitable for producing a significant yield of the corresponding high Z heavy partners. This projectile and tar-

get combination was already used in previous measurements mainly focused on neutron transfer [1,10,11] and/or on strongly damped collisions [1,12].

We then felt interesting to measure, for the same system, the final mass and charge yields of light reaction products, differential and total cross sections, total kinetic energy losses and the survival probability against fission of the Pb-like fragment. All these experimental quantities are compared here with semiclassical models [13,14] that solve in an approximate way the system of coupled equations including surface collective modes, single- and two-nucleon transfer modes. The survival probability against fission of the heavy reaction products is also computed within the same model and compared with the experimental data.

In Sec. II we present the setup and the details of the experiment. In Sec. III we discuss the experimental results, and in Sec. IV we compare data with model calculations. Conclusions are drawn in Sec. V.

II. THE SETUP AND EXPERIMENT

The experiment was done with the Tandem+ALPI booster of the Laboratori Nazionali di Legnaro. A ^{58}Ni beam was accelerated onto a ^{208}Pb target at the bombarding energy of $E_{lab}=328.4$ MeV, corresponding to $\simeq 3\%$ above the Coulomb barrier. The target had a thickness of 200 μg/cm^2 and an isotopic enrichment of 99.8%, and was sandwiched between two 15 μg/cm^2 C foils. Light reaction products were detected with the time-of-flight (TOF) spectrometer PISOLO [5,15], while the associated heavy partners produced in the binary reactions were detected in kinematic coincidence using a transmission-type multiwire parallel-plate avalanche counter (MWPPAC).

PISOLO combines a large solid angle and good mass (A)
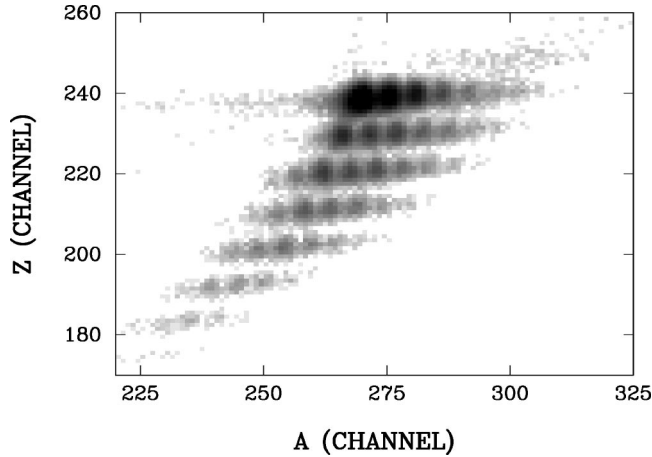
FIG. 1. A-Z matrix at $\theta_{\text{lab}} = 90°$. The most intense spot corresponds to $Z = 28, A = 58$.

and nuclear charge (Z) resolutions for ions with $A \leq 100$ at energies ≥ 1 MeV/amu. TOF signals were derived from two microchannel-plate (MCP) detectors placed at a distance of $\simeq 3.5$ m between each other, while Z and total energy signals were obtained with a multi anode transverse field ionization chamber. Between the MCP, two doublets of magnetic quadrupoles are placed with a resulting effective solid angle of $\simeq 3$ msr. An example of A-Z matrix obtained with the spectrometer at the grazing angle $\theta_{\text{lab}} = 90°$ is shown in Fig. 1. One can observe transfer channels up to the pickup of eight neutrons $(+8n)$ and the stripping of eight protons $(-8p)$. The average mass and nuclear charge resolutions are $\Delta A / A \simeq 1/100$ and $\Delta Z / Z \simeq 1/60$, respectively.

The transmission of the spectrometer was determined from the yield of quasielastic events as a function of the magnetic fields of the quadrupoles. The ratio of the yields with the quadrupole fields switched on and off turns out to be $\simeq 13.7$, this giving directly the effective solid angle of the instrument. For more details see Refs. [5,15].

Absolute normalization of the cross sections and relative normalization between different runs were ensured by four silicon monitor detectors placed in the sliding-seal scattering chamber connected to the spectrometer. The MWPPAC for the detection of the heavy partners is an improved version of the one described in Refs. [16,17]. It has an area of 8×8 cm^2 and consists of a central cathode (providing timing signals) between two X and Y grids (providing position signals through the delay line method). Timing and position resolutions are $\simeq 350$ ps and 1 mm (for both X and Y), respectively. The MWPPAC was positioned with its active surfaces perpendicular to the reaction plane and at a distance of $\simeq 30$ cm from the target, as a compromise between solid angle, high rate capabilities and angular resolution needs. The covered angular range was $\simeq 15°$ both in-plane and out-of-plane, and the solid angle was $\simeq 70$ msr, sufficient to detect all the relevant coincident heavy partners produced in the multinucleon transfer process. The intrinsic efficiency of the MWPPAC was 100% for the detected ions over the whole surface.

In Fig. 2 (left side) we show the X and Y position spectra for the events ungated and gated by the TOF spectrometer. The largest fraction of the coincident events are due to the elastically scattered ^{208}Pb ions, and the width of the peak is mainly determined by the spectrometer angular integration of $\simeq 1.5°$. In the right side of the same figure we show the X spectra with software gates made on specific Z,A events for the light partner (identified with the spectrometer). One sees the kinematic shift of the peaks towards more forward angles as more nucleons are transferred, as expected from the different reaction Q values involved.

From the ratio of the events detected in coincidence between the spectrometer and the MWPPAC and those with the spectrometer in singles we could extract what we define the average survival probability against fission P_s of the heavy fragment. P_s was obtained by gating on each specific Z and A of the light products and getting the corresponding events in the MWPPAC produced in the binary reaction. From the kinematics of the reaction it turns out that the average ve-
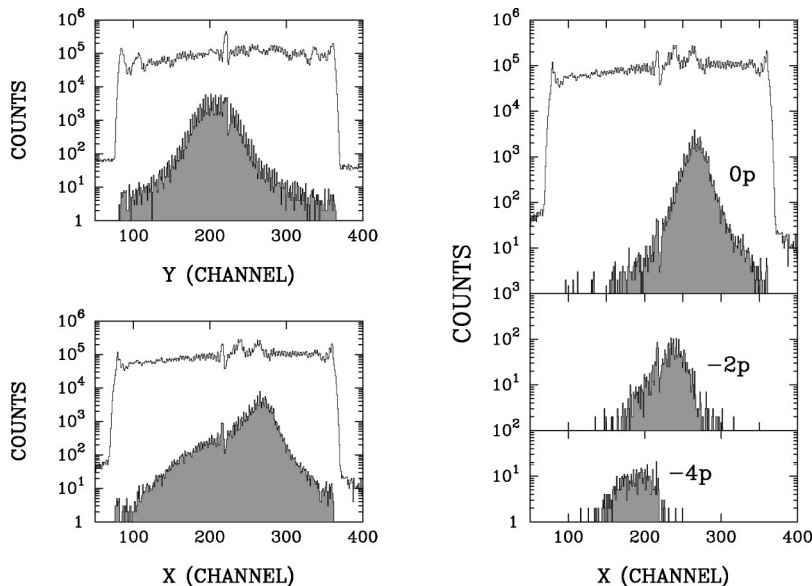
FIG. 2. X and Y position event distributions in the MWPPAC. Left side: ungated (near square shape) and gated (shaded areas) over all transfer events detected with the spectrometer. Right side: ungated and gated for specific transfer channels. Calibration of the spectra is $0.05°$/channel.
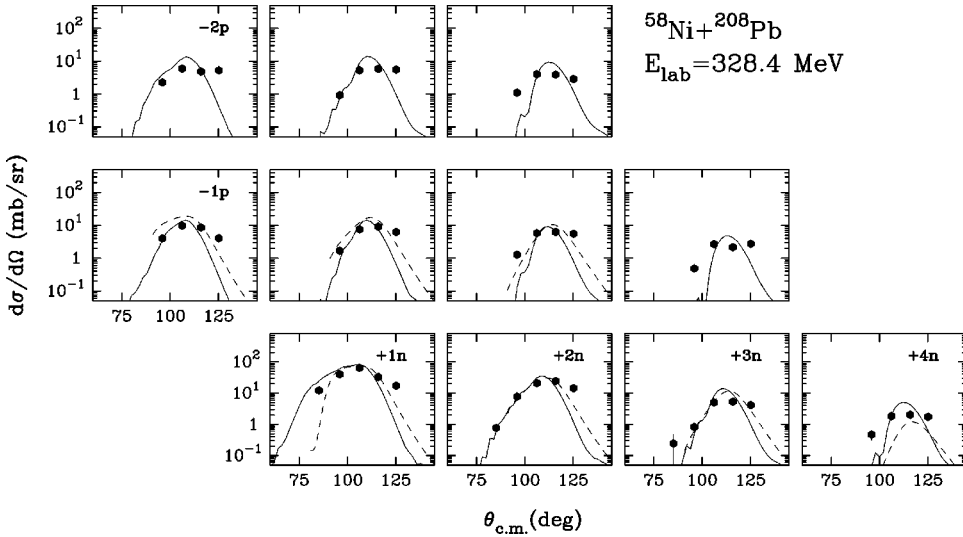
FIG. 3. Experimental (dots) and theoretical (lines) Q value integrated angular distributions for some representative transfer channels. The full lines are the CWKB calculations and the dashed lines are the GRAZING predictions (shown for selected cases). Experimental errors include the statistical and systematic ones. The cross sections for the different channels are laid out in a $(\Delta N, \Delta Z)$ matrix.

locities of the heavy ejectiles (in the lab system) and those of the fission fragments (in the c.m. of the heavy fissioning nuclei) are quite similar and have values $\simeq 1.3$ cm/ns. Taking also into account the geometry of the experiment, the fraction of fission products from the heavy fragments in coincidence with PISOLO and going into the MWPPAC is estimated to be $\simeq 2\%$, therefore corrections to the original experimental ratios were not done.

III. EXPERIMENTAL RESULTS

Angular distributions were measured in the laboratory angular range $70°–110°$ that covers most of the total transfer flux. For some representative transfer channels angular and total kinetic energy loss (TKEL) distributions are shown in Figs. 3 and 4, respectively. The TKEL are derived assuming a pure binary process and no correction has been applied for reconstructing the primary distributions. From Fig. 4 one sees that the distributions for pure neutron pick-up channels have their major contribution close to the optimum Q values ($Q \simeq 0$ MeV), with a tail extending towards larger TKEL as more neutrons are transferred. This trend is quite similar for

channels that involve the transfer of protons with the large TKEL tail becoming more and more pronounced. These features are almost angle independent and confirm the general evolution of the reaction already observed for other systems [5,6] and show that even at energies close to the Coulomb barrier large energy losses take place [13].

The total cross sections obtained by integrating the measured angular distributions are reported in Fig. 5. For channels involving the stripping of few protons the isotopic distributions extend mainly along the neutron pick-up chain, but as more protons are transferred the neutron flux tends to shift in the stripping direction. Since for the present system optimum Q-value arguments favor the pick-up of neutrons and the stripping of protons, the trend observed in the data may be attributed, at least partly, to the effect of neutron evaporation from the primary fragments. Indeed, we plot in Fig. 6 the total cross sections, now as a function of the transferred number of protons (ΔZ), for channels involving neutron pickup (left side) and neutron stripping (right side). It is evident that cross sections for neutron pickup channels decrease very smoothly as a function of the number of transferred protons, while neutron stripping channels have a very
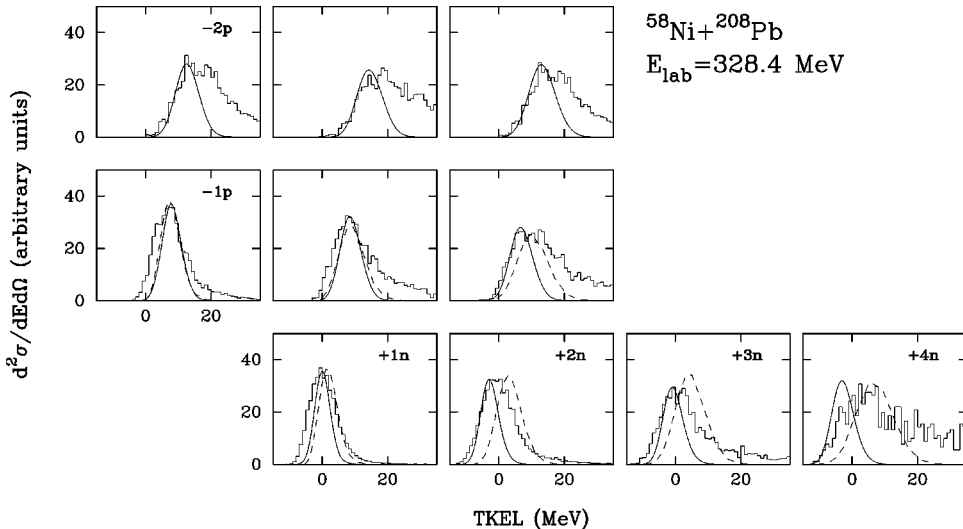
FIG. 4. Experimental (histograms) and theoretical (lines) total kinetic energy loss (TKEL) distributions at $\theta_L = 90°$ for some representative transfer channels. The full lines are the CWKB calculations and the dashed lines are the GRAZING predictions (shown for selected cases). The spectra for the different channels are laid out in a $(\Delta N, \Delta Z)$ matrix.
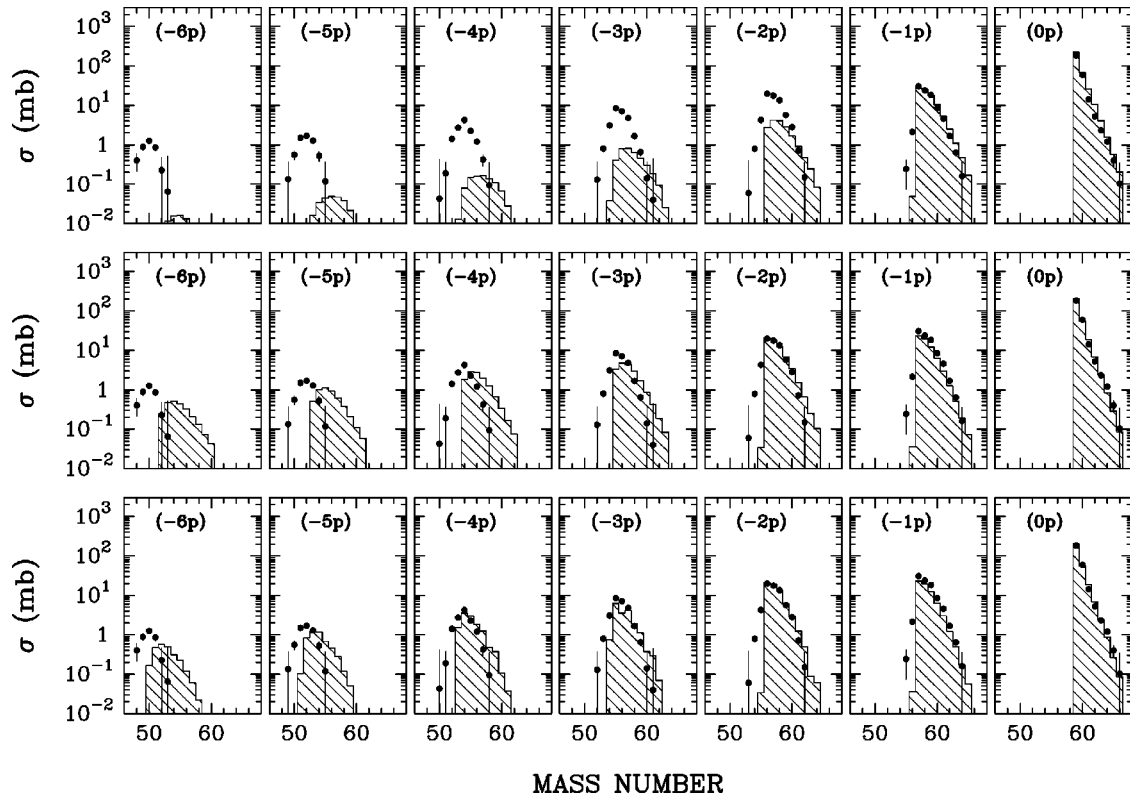
FIG. 5. Total angle and *Q*-value integrated cross sections for the transfer channels observed. Points and histograms are the experimental and theoretical values, respectively. Experimental errors include the statistical and systematic ones. The calculations shown in the top row include only single nucleon transfer modes, those in the middle row have in addition a proton pair mode, and in the bottom row also evaporation effects are taken into account (see text).

different behavior, indicating that two kinds of reaction mechanisms are involved. While the neutron pickup trend supports the idea of a direct population in terms of an independent transfer of neutrons and protons, the neutron stripping side shows a strong influence of some other mechanism that we identify with neutron evaporation. This difference between pickup and stripping of neutrons was also observed,
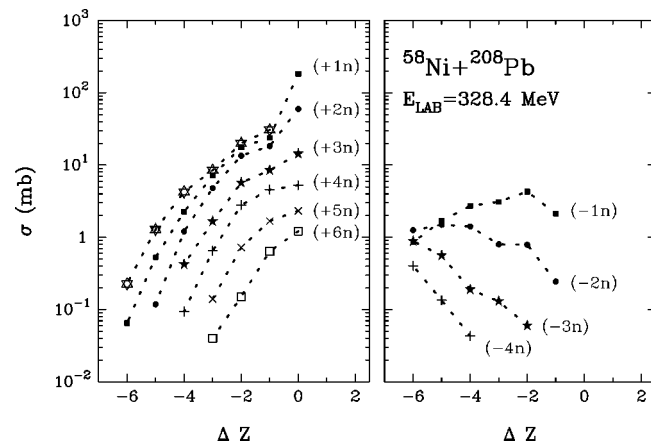
FIG. 6. Total experimental cross sections for channels involving pickup (left side) and stripping (right side) of neutrons, as a function of the number of transferred protons ΔZ. The open stars on the left part are the pure proton transfer channels.

even in a more marked way, in the study of the ^{64}Ni $+^{238}$U system [5].

As discussed in the previous section, from the experimental ratios between coincidences and singles with the spectrometer we could obtain the survival probability against fission (P_s) of the heavy fragments. We observed that the P_s values have little dependence, for a specific Z, on the number of transferred neutrons. In Fig. 7 we then plot P_s as a function of the number of transferred protons ΔZ, averaged over the neutron numbers, together with the calculations described in the following section. One sees that P_s is close to 1 up to the transfer of $\simeq 3$ protons, then a significant deviation occurs for $\Delta Z \leqslant -4$ with an increase of the fission probability as more protons are transferred. It turns out that the present P_s values are very similar to the ones quoted in Ref. [12], where the study was performed at a center of mass energy $\simeq 80$ MeV above the Coulomb barrier.

IV. COMPARISON WITH CALCULATIONS

The data are analyzed using the semiclassical Complex WKB (CWKB) model, described in Ref. [14]. The model is well suited for the study of transfer reactions at Coulomb barrier energies and was already successfully used in the comparison with experimental data for various systems [6,17,18]. The formalism involves the same approximations which were used to calculate the absorptive [19] and polar-
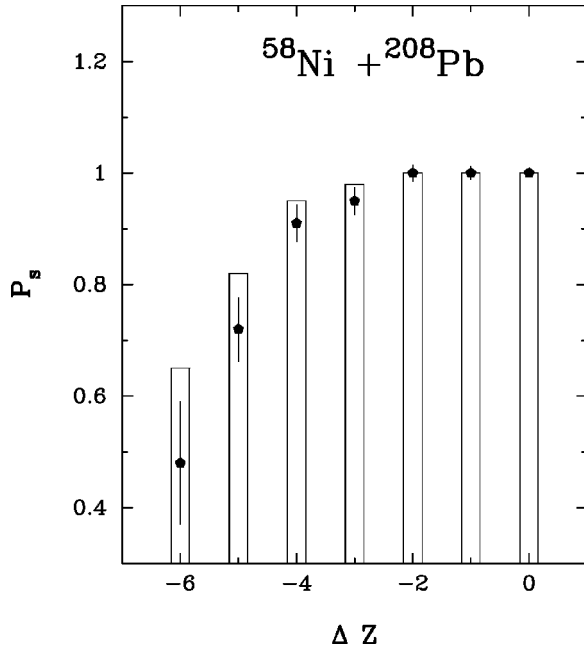
FIG. 7. Survival probability against fission P_s for the heavy targetlike fragments as a function of the number of transferred protons ΔZ (detected with the spectrometer) averaged over neutron numbers. Points and histograms are the experimental and theoretical values, respectively. Experimental errors are only the statistical ones.

ization [20,21] components of the optical potential and the off-diagonal inelastic couplings. The model was first developed to deal with one-particle transfer [14,17] and later generalized to compute cross sections of multinucleon transfer channels via a sequence of single nucleons and of pair modes. The nucleon pair degrees of freedom are included in the calculation by using a macroscopic formfactor [18]. We refer to the cited references for details.

We employ the single-particle levels of projectile and target (for neutrons and protons) as shown in Fig. 8 to calculate the single particle formfactors which constitute the main ingredients for the determination of the transfer amplitudes. In order to cover the full range of Q values one has to include all single-particle levels above the Fermi surface and a full shell below. Hence, some other levels are obtained by diagonalizing a shell model potential (we used the Stockholm parametrization [22]) and added to the experimental single-particle levels obtained with the standard procedure from the binding energies and spectra of neighboring nuclei. For the case of neutrons in nickel, the states are treated as quasiparticle and quasihole states, and this is the reason why the $2p_{3/2}$ level appears twice in Fig. 8 (the Fermi energy is here represented by a broken line).

For the real part of the optical potential we used a Woods-Saxon form with the parameters from the empirical potential of Ref. [23] (we recall that this empirical potential was obtained from a best fit procedure over many elastic scattering data) and for the imaginary part we kept the same geometry with a strength reduced to 1/3 of the real part.

In the top row of Fig. 5, we show (histograms) the calculated total cross sections for all relevant mass and charge partitions, in comparison with experimental data. All single-nucleon transfer modes, compatible with the above choice of single-particle levels, are used. The multinucleon transfer are calculated in a successive approximation considering all the transitions as independent. A good agreement between data and theory is obtained for the transfer of pure neutrons and for channels involving the stripping of one proton ($-1p$). Noteworthy is the fact that the shape of the mass yield for the ($-1p$) case is very well reproduced on the neutron pick-up side. As more protons are transferred the calculations are not able to follow the trend of the data which tend to develop a population on the light isotope side.

The data were also compared with the results of the program GRAZING [24] based on the semiclassical model developed in Ref. [13]. The model treats on the same footing quasielastic and deep inelastic processes and describes the transfer reaction as a sequence of independent single-nucleon transfer modes; nucleon evaporation from the primary fragments is also taken into account in a simple way. The model was already successfully applied in the comparison of different multinucleon transfer data [5,6] and, recently, of fusion excitation functions and barrier distributions [25]. The total cross sections obtained with GRAZING for the present system are in quantitative agreement with the ones calculated with the CWKB model and are not reported in the figure (for the angular distributions and excitation energy spectra see the corresponding figures discussed below).

The discrepancies between data and calculations may indicate that degrees of freedom beyond single-particle transfer modes have to be incorporated in the theory or, as pointed out in the previous section, that more complex processes play an important role. In order to understand which important degrees of freedom are missing in our treatment, we show in Fig. 9 the total cross sections for pure proton transfer (left side) and pure neutron transfer (right side). For pure proton transfer the results of the calculation are shown with a dotted line. It is clear from this figure that the neutron channels are well described by a sequence of single-neutron transfers while, starting from the ($-2p$) channel, the protons are strongly underestimated. It is thus natural to try adding a new degree of freedom, namely, the transfer of a pair of protons. This may be easily incorporated in the CWKB model by using the macroscopic form factor

$$f_p(r) = \beta_p \frac{dV(r)}{dr}, \qquad (1)$$

where $V(r)$ is the optical potential and β_p is a deformation parameter that measures the collectivity of the mode. In principle, one should use several pair transfer modes with different Q values and different angular momentum transfer λ, but, to reduce the number of parameters, we decided to include one pair transfer mode at the optimum Q value and for $\lambda = 0$. Fixing the β_p parameter to reproduce the pure $-2p$ channel we obtain the results shown as a dashed line in Fig. 9 for pure proton transfer and in the middle row of Fig. 5 for the full isotopic distribution. It is interesting to notice that once the yield of the ($-2p$) channels are reproduced, the predictions for the other charge transfer channels are also
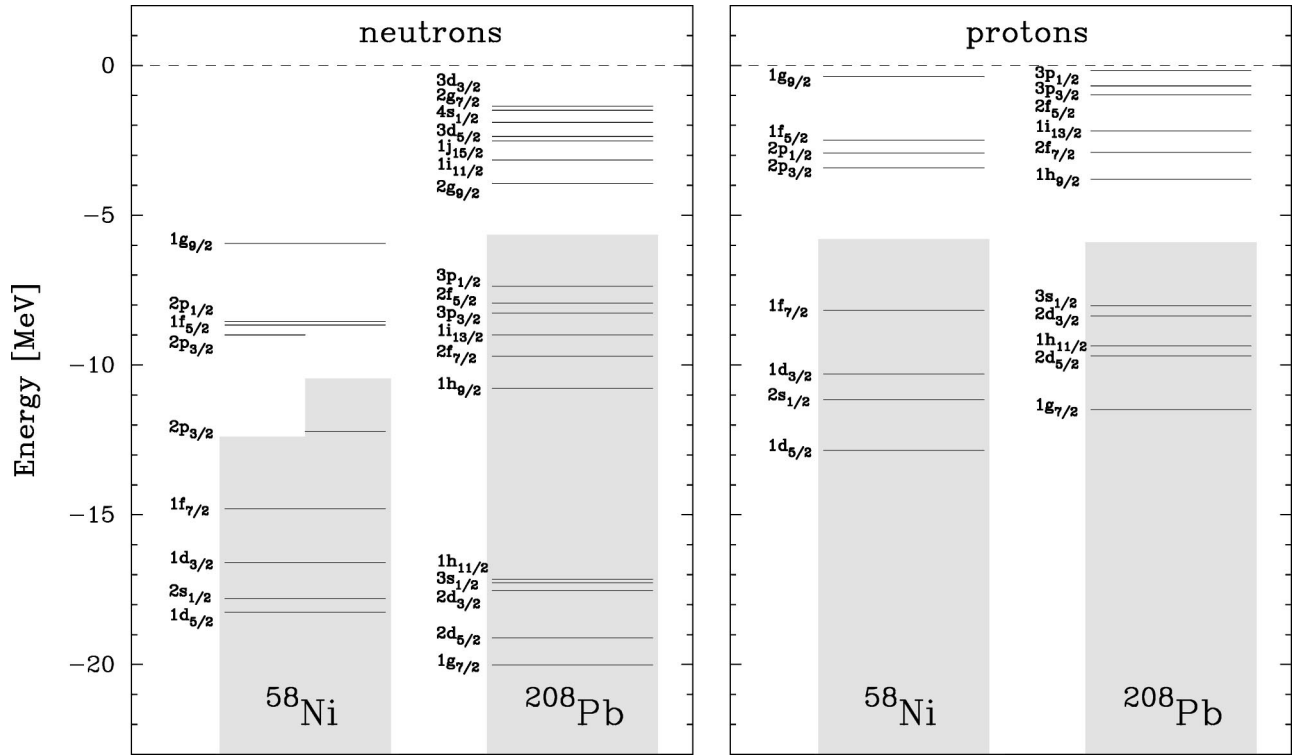
FIG. 8. Single-particle levels for projectile and target. The shaded areas indicate the occupied levels.

much better indicating that the proton pair mode may be an important degree of freedom in the transfer process. Its treatment is, at present, only at a phenomenological level and it is difficult to relate microscopically its strength to the pair correlations in target and in projectile (both enter in the definition of the form factor).
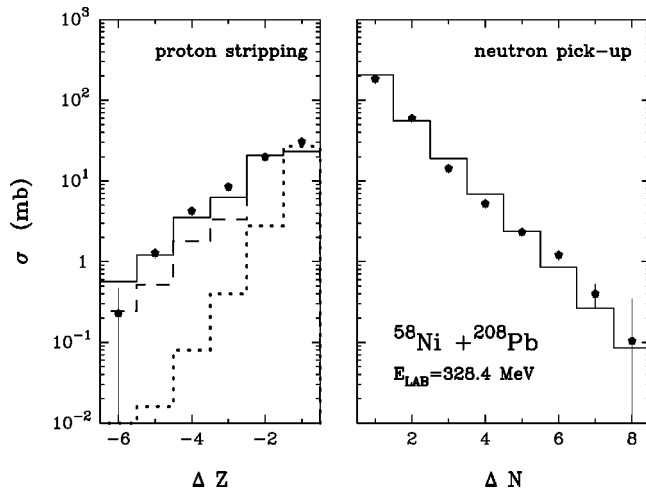
FIG. 9. Total cross sections for pure proton stripping (left side) and pure neutron pickup (right side) channels. The dotted line is the CWKB calculation including single nucleon transfer modes. The dashed line represents the result with an additional two-proton pair mode and the solid line includes also the effect of nucleon evaporation from the primary fragments. For the pure neutron transfer no pair transfer was included and the cross section represented by the dashed and the dashed-dotted lines (not shown) are very close to the full line.

In Figs. 3 and 4 we report the CWKB calculations (full lines), including both single nucleon and proton pair transfer modes, for the angular distributions and TKEL, respectively. The experimental angular distributions are quite well reproduced by the theory, both in absolute scale and in shape. In the same figures, for selected channels, we report the results of the code GRAZING. In Fig. 3, one sees that the predictions of GRAZING (dashed lines) for the cases involving pure neutron and $(-1p)$ transfer channels give very similar results as those based on the CWKB theory. The TKEL are calculated for a specific partial wave and not at a specific angle for which the contribution of several partial waves are important. This may easily explain why in the TKEL spectra we are missing strength at large energy losses.

As observed in the figure the transfer strength extends to quite high excitation energies, therefore the final yield can be considerably altered by evaporation. To estimate the effect of the evaporation on the fragment distribution, we first extracted the excitation energy and final angular momenta of the different light and heavy products from the CWKB model. These values, for each Z and A, were then used as inputs in the evaporation code PACE2 [26], which provides the final mass and charge partitions computing the evaporation of nucleons according to the statistical model. Using the default parameters of PACE2, the final cross sections obtained for the light fragments are shown in the bottom row of Fig. 5. Here one sees that the theoretical mass distributions are now closer to the data, especially for the cases of many transferred protons. In particular the pure proton transfer channels, shown with a full line in Fig. 9, are very well reproduced.

Calculations with PACE2 was also performed for the heavy transfer products adopting the same procedure as for the light partners. In this case we were interested in the survival probability against fission, which is the quantity to be compared with the experimentally derived P_s. In Fig. 7, the experimental and theoretical values are shown for the different heavy partners produced via proton stripping reactions. The overall agreement between data and theory is good, considering that no attempt has been done to fit the data by varying the parameters.

V. CONCLUSIONS

Multinucleon transfer reactions in ^{58}Ni$+^{208}$Pb were studied at $E_{lab}=328.4$ MeV. The final mass, charge and Q-value distributions of light reaction products were measured with a time-of-flight spectrometer, and the survival probabilities of the associated heavy fragments were obtained via a high resolution kinematic coincidence. The experimental observables, i.e., mass and charge yields, differential and total cross sections, total kinetic energy losses and fission survival prob-

abilities, were compared with semiclassical models, which give an overall good description of the data.

The inclusion of a proton pair mode, by using a phenomenological form factor, in addition to the transfer of independent nucleons allows a much better description of the data. This indicates that pair modes may constitute an important degree of freedom in the transfer process, but much more experimental and theoretical efforts are needed in order to fully understand its consequences both from the reaction and structure point of view. The experimental values of the survival probabilities of the heavy fragments show that in selected cases multinucleon transfer via proton stripping may be effective in populating high Z heavy nuclei.

[1] K. Sapotta, R. Bass, V. Hartmann, H. Noll, R.E. Renfordt, and K. Stelzer, Phys. Rev. C **31**, 1297 (1985).

[2] K.E. Rehm, Annu. Rev. Nucl. Part. Sci. **41**, 429 (1991).

[3] C.L. Jiang, K.E. Rehm, J. Gehring, B. Glagola, W. Kutschera, M. Rhein, and A.H. Wuosmaa, Phys. Lett. B **337**, 59 (1994).

[4] C.L. Jiang, K.E. Rehm, H. Esbensen, D.J. Blumenthal, B. Crowell, J. Gehring, B. Glagola, J.P. Schiffer, and A.H. Wuosmaa, Phys. Rev. C **57**, 2393 (1998).

[5] L. Corradi, A.M. Stefanini, C. Lin, S. Beghini, G. Montagnoli, F. Scarlassara, G. Pollarolo, and A. Winther, Phys. Rev. C **59**, 261 (1999).

[6] L. Corradi, A.M. Vinodkumar, A.M. Stefanini, D. Ackermann, M. Trotta, S. Beghini, G. Montagnoli, F. Scarlassara, G. Pollarolo, F. Cerutti, and A. Winther, Phys. Rev. C **63**, 021601(R) (2001).

[7] W. von Oertzen and A. Vitturi, Rep. Prog. Phys. **64**, 1247 (2001).

[8] W. von Oertzen, Z. Phys. A **342**, 177 (1992).

[9] W. von Oertzen, in *Heavy Elements and Related New Phenomena*, edited by W. Greiner and R.K. Gupta (North Holland, Amsterdam, 1999).

[10] M. Beckermann, R.L. Auble, F.E. Bertrand, J.L. Blankenship, B.L. Burks, C.W. Glover, R.O. Sayer, G.R. Satchler, D. Shapira, and R.L. Varner, Phys. Rev. Lett. **58**, 455 (1987).

[11] K.E. Rehm, D.G. Kovar, W. Kutschera, M. Paul, G. Stephans, and J.L. Yntema, Phys. Rev. Lett. **51**, 1426 (1983).

[12] M.B. Chatterjee, S.P. Baldwin, J.R. Huizenga, D. Pade, B.M. Quednau, W.U. Schröder, B.M. Szabo, and J. Töke, Phys. Rev. C **44**, R2249 (1991).

[13] A. Winther, Nucl. Phys. **A572**, 191 (1994); **A594**, 203 (1995).

[14] E. Vigezzi and A. Winther, Ann. Phys. (N.Y.) **192**, 432 (1989).

[15] G. Montagnoli, F. Scarlassara, S. Beghini, A. Dal Bello, G.F. Segato, A.M. Stefanini, D. Ackermann, L. Corradi, J.H. He, and C.J. Lin, Nucl. Instrum. Methods Phys. Res. A **454**, 306 (2000).

[16] S. Beghini, L. Corradi, J.H. He, and A. Dal Bello, Nucl. Instrum. Methods Phys. Res. A **362**, 526 (1995).

[17] L. Corradi, G. de Angelis, A. Gadea, G. Maron, D.R. Napoli, A.M. Stefanini, S. Beghini, D. Bazzacco, G. Montagnoli, P. Pavan, F. Scarlassara, C.A. Ur, J.H. He, C. Fahlander, G. Pollarolo, and F. Cerutti, Phys. Rev. C **61**, 024609 (2000).

[18] L. Corradi, A.M. Stefanini, D. Ackermann, S. Beghini, G. Montagnoli, C. Petrache, F. Scarlassara, C.H. Dasso, G. Pollarolo, and A. Winther, Phys. Rev. C **49**, R2875 (1994).

[19] R.A. Broglia, G. Pollarolo, and A. Winther, Nucl. Phys. **A361**, 307 (1981).

[20] G. Pollarolo, R.A. Broglia, and A. Winther, Nucl. Phys. **A406**, 369 (1983).

[21] C.H. Dasso, S. Landowne, G. Pollarolo, and A. Winther, Nucl. Phys. **A459**, 134 (1986).

[22] J. Blomqvist and V. Wahlborn, Arkiv Fys. K. Svenska Vetensk. **16**, 545 (1960).

[23] Ö. Akyüz and A. Winther, in *Nuclear Structure and Heavy-Ion Physics*, Proceedings of the International School of Physics "Enrico Fermi," Course LXXVII, Varenna, edited by R.A. Broglia and R.A Ricci (North Holland, Amsterdam, 1981).

[24] A.Winther, program GRAZING (unpublished).

[25] G. Pollarolo and A. Winther, Phys. Rev. C **62**, 054611 (2000).

[26] A. Gavron, Phys. Rev. C **21**, 230 (1980).